3-2001

Hubble Space Telescope Images of the Ultraluminous Supernova Remnant Complex in NGC 6946

William P. Blair
Johns Hopkins University

Robert A. Fesen
Dartmouth College

Eric M. Schlegel
Harvard-Smithsonian Center for Astrophysics

THE ASTRONOMICAL JOURNAL, 121:1497–1506, 2001 March

HUBBLE SPACE TELESCOPE IMAGES OF THE ULTRALUMINOUS SUPERNOVA REMNANT COMPLEX IN NGC 6946[1]

WILLIAM P. BLAIR
Department of Physics and Astronomy, Johns Hopkins University, 3400 North Charles Street, Baltimore, MD 21218-2686; wpb@pha.jhu.edu
ROBERT A. FESEN
Department of Physics and Astronomy, Dartmouth College, 6127 Wilder Laboratory, Hanover, NH 03755-3528; fesen@snr.dartmouth.edu
AND
ERIC M. SCHLEGEL
Harvard-Smithsonian Center for Astrophysics, 60 Garden Street, Cambridge, MA 02138; eschlegel@cfa.harvard.edu
Received 1999 September 4; accepted 2000 November 20

ABSTRACT

We present *Hubble Space Telescope* (*HST*) narrow-passband Hα and [S II] images and broadband continuum images of the region around an extremely luminous optical and X-ray supernova remnant complex in the spiral galaxy NGC 6946. These images, obtained with the PC1 CCD of the Wide Field Planetary Camera 2, show a circular, limb-brightened shell of diameter 0.″35 [9 *d*/(5.1 Mpc) pc] superposed on the edge of a larger, lower surface brightness elliptical shell (1.″4 × 0.″8, or ≃34 pc × 20 pc). The *HST* images allow us to see that the [S II]:Hα ratio remains high across both shells, indicating that both are collisionally heated. A brightening of the Hα and [S II] line emission arises on the eastern side of the smaller shell, where it is apparently interacting with the western edge of the larger shell. Our *HST* *V* image includes the nebula's strong [O III] λ5007 emission in the blue wing of the filter, providing a glimpse at the [O III] nebular morphology. The smaller shell looks similar, but the extended structure looks sharper than in Hα and [S II] images, reminiscent of a cavity wall. The *HST* and ground-based continuum images show the brightest members of the underlying and adjacent stellar population, indicating the presence of massive OB stars in and near the region. A new optical ground-based spectrum confirms that the [N II]:Hα ratio is enhanced in the region, consistent with mass loss from massive stars. These data show an average ([S II] λλ6716, 6731):Hα ratio across both shells of ∼1 and a mean electron density of ∼400 cm^{-3}, indicating preshock densities of order 10 cm^{-3}. We interpret this nebular morphology and supporting information as an indication of multiple supernova explosions in relatively close temporal and spatial proximity. We discuss possible scenarios for this complex region and the reasons for its extreme luminosity.

Key words: galaxies: individual (NGC 6946) — supernova remnants

1. INTRODUCTION

The face-on spiral galaxy NGC 6946 [SAB(rs)cd, de Vaucouleurs, de Vaucouleurs, & Corwin 1976; $d = 5.1$ Mpc, de Vaucouleurs 1979] has generated at least six supernovae (SNe) in the last 85 years. This rate is rivaled only by M83, also a face-on Scd galaxy, which has had six recorded SNe (see Cowan & Branch 1985 and references therein; also Liller 1990). Both NGC 6946 and M83 show evidence of active star formation and starburst activity, with at least some of the observed SNe presumably arising from young, massive stars.

With so many historical SNe seen in these two galaxies, a large number of young supernova remnants (SNRs), perhaps older than the historical record but still relatively young, might be expected to be present. Some of these young SNRs might still be in the relatively brief (≤2000 yr) "ejecta dominated" phase, like the luminous SNR in NGC 4449 (Blair, Kirshner, & Winkler 1983). Such considerations motivated us to undertake deep ground-based CCD imaging surveys of NGC 6946 and M83 using interference-filter images to search systematically for young optical SNR candidates.

In the course of an imaging survey of NGC 6946, an extraordinarily bright optical SNR was discovered (Blair & Fesen 1994) within the error circle of a bright *ROSAT* Position Sensitive Proportional Counter source having a luminosity of $L_X(0.2\text{–}3\ \text{keV}) \sim 3 \times 10^{39}$ ergs s^{-1} (Schlegel 1994). This object is listed as No. 16 in a subsequent optical SNR survey of NGC 6946 (Matonick & Fesen 1997; hereafter the object will be designated MF 16) and is several times brighter than any of the other 26 SNRs they identified. VLA observations show MF 16 to be a powerful radio source, several times brighter than the young, Galactic SNR Cas A, indicating a probable interaction with dense circumstellar or interstellar material (Van Dyk et al. 1994). In fact, the large observed X-ray, optical, and radio luminosities initially suggested a relatively youthful, ejecta-dominated remnant similar to the NGC 4449 SNR mentioned above. However, a moderate-resolution optical spectrum (Blair & Fesen 1994) showed no evidence of either high velocities or peculiar abundances. Furthermore, the VLA observation resolved the source at 6 cm at about 1″, or 25 *d*/(5.1 Mpc) pc. Collectively, these observations indicated that the object is an unusually luminous but otherwise normal, average-size, interstellar medium–dominated SNR.

We have used the Wide Field Planetary Camera 2 (WFPC2) on the *Hubble Space Telescope* (*HST*) to obtain high-resolution images of the region surrounding the unusually luminous SNR in NGC 6946. We have also

[1] Based on observations with the NASA/ESA *Hubble Space Telescope*, obtained at the Space Telescope Science Institute, which is operated by the Association of Universities for Research in Astronomy, Inc., under NASA contract NAS 5-26555.

obtained deeper ground-based optical spectra of the SNR. These new observations are reported in the next section, followed by a discussion of possible interpretations of this remarkable region. Our conclusion, based primarily on the observed morphology of the emission, is that MF 16 is actually a small region, containing multiple SNRs, in which a relatively youthful SNR is currently interacting with the shell of an older, neighboring SNR. However, the tremendous luminosity of the region arises not only from the interaction region between the two SNRs but also from the dense surroundings into which the shock fronts are expanding.

2. OBSERVATIONS AND REDUCTIONS

2.1. *HST Imaging*

CCD images of NGC 6946's northeastern section, which contains the unusually luminous SNR complex, were obtained on 1996 January 27 with WFPC2 aboard *HST*. The SNR was positioned near the center of the PC1 CCD to provide both good resolution and sufficient field coverage to assess its local environs. Filters and exposure times were Hα F656N (2×700 s), [S II] F673N (2×1100 s), *V*-band F555W (400 s), and *B*-band F439W (2×400 s). There was only one F555W exposure because the exposure was shorter than the default exposure time for the CR-SPLIT optional parameter to be invoked automatically. Unfortunately, having only a single exposure makes cosmic-ray removal problematic.

The broadband *B* and *V* images were intended to provide a continuum band for comparison against the emission-line images, as well as color information on the underlying stellar population in the region to be studied. In reality, the *B*-band data show only modest detections of the brightest stars in the region, and the nebular emission from the SNR (primarily from [O III] λ5007) was sufficiently bright to be recorded on the F555W exposure in addition to the stars. The observations were planned so that the three WFC CCDs would be placed on the bright northern spiral arm of NGC 6946, allowing a search for other SNRs using the [S II]:Hα ratio (see Long et al. 1990; Blair & Long 1997). The results of our analysis of this portion of the observations will be reported separately. Here we report exclusively on the emissions detected with the PC1 CCD.

Data reductions used the calibrated data extracted from the Guest Observer tape provided by the STScI, using tasks available in the IRAF/STSDAS environment.[2] Images were checked for accurate alignment and then exposure pairs (where available) were combined with the task CRREJ, removing the bulk of the cosmic rays (although some isolated, hot camera pixels remain). For the single F555W image, the region surrounding the SNR was manually cleaned using IRAF's IMEDIT task; the image was carefully checked against the other frames to avoid removal of real features. However, because the F555W exposure was the "deepest" available for showing the stellar component, it was not always possible to make a clear determination.

Figure 1 shows an aligned 18″ region including the ultraluminous SNR (*left below center of each panel*) and its environs in all four bandpasses. In Figures 1–5, north is to the upper right and east to the upper left, as in the original *HST* data sets. An OB association and its H II emission can be seen at the lower right in Figure 1, and another SNR (MF 15) identified by Matonick & Fesen (1997) and mentioned by Blair & Fesen (1994) is at the upper right. Although the stretch in Figure 1 is performed to show the faintest emissions detected, the tremendous relative surface brightness of MF 16 (about 10 times as bright as MF 15 at Hα) is obvious.

For comparison with the *HST* data and to provide context, in Figure 2 we show "postage stamps" of ground-based CCD images of the region, from the imaging data reported by Blair & Fesen (1994). The four bandpasses shown are Hα, [S II], [O III], and a red continuum band centered at 6100 Å. The images are rotated to match the *HST* data, and the region shown is 21.″6 square, slightly larger than the region shown in Figure 1. The left panels show a "soft stretch," making it easy to correlate features against the *HST* images, and the right panels are contrast-enhanced to show fainter structures not visible in the *HST* images. Although MF 16 is saturated, note the appearance of the second SNR (MF 15) at upper right, the brightness and extent of the H II emission associated with the OB association at lower right, and the presence of distinct continuum emission at and adjacent to the location of MF 16 itself. At least the brightest of the stars contributing to this emission are visible in the *HST* images. These data will be discussed further in § 3.

Because only one image was available with the F555W filter, we show "before" and "after" images of the region directly around MF 16 in Figure 3. While most of the cosmic rays are obvious in the top panel and are cleaned out very well with the IMEDIT task of IRAF, the reader should note that a couple of cosmic rays that affect the SNR shell directly cannot be corrected for without uncertainty. Because of the low level of detection of MF 16 in the F555W exposure, this could have a minor residual affect on the appearance of this region.

In Figure 4, we show a 3″ region centered directly on MF 16 from all four of the *HST* images, with the contrast set to show the overall structure of the region. The Hα and [S II] images show very similar morphologies, dominated on the west by a bright crescent of emission that is part of a small circular ring and on the east by a larger structure with lower surface brightness and, possibly, multiple loops. In F555W, the small ring is more uniform in brightness but positionally coincident with the ring seen in Hα and [S II]. The larger structure, however, looks quite different, showing a more elliptical shape, possibly with a sharper edge. The presence of a star squarely in the extended structure, as seen in the F555W exposure and confirmed by the F439W image, may affect this comparison.

Because the appearance in Hα and [S II] is so similar, we have added these images together to increase the signal-to-noise ratio (S/N). We have also used the MAGNIFY task in IRAF to subsample the summed data and the F555W data by a factor of 2 to reduce the visual appearance of pixelation. Figure 5 displays these two images for comparison. It is clear that the star within the shell is just barely detected in the narrowband summed image, but it does not significantly contaminate the image. Figure 5 also introduces some nomenclature we will use in the discussion below.

[2] IRAF is distributed by the National Optical Astronomy Observatories, which are operated by the Association of Universities for Research in Astronomy, Inc., under cooperative agreement with the National Science Foundation. The Space Telescope Science Data Analysis System (STSDAS) is distributed by the Space Telescope Science Institute (STScI).

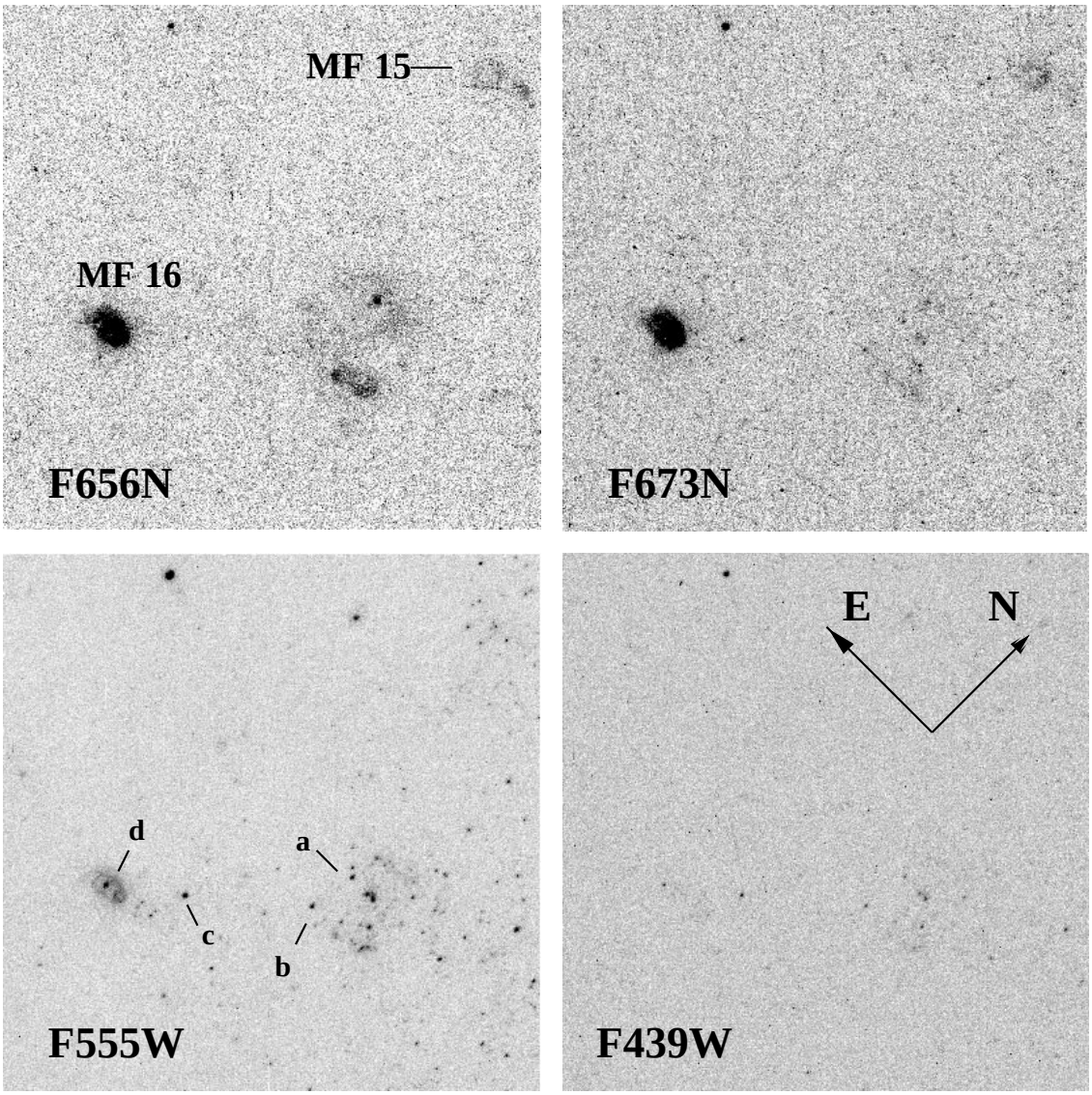

FIG. 1.—*HST* WFPC2 images of a 17.″94 square region near MF 16, from the PC1 chip. *Top left*, F656N (Hα); *top right*, F673N ([S II]); *bottom left*, F555W (approximate *V*-band continuum); *bottom right*, F439W (*B*-band continuum). The scaling has been set to show the faintest features detected, so MF 16 (bright object, *lower left*) appears saturated. (MF 16 is seen in F555W because of bright [O III] λ5007 nebular emission passed by the broad filter.) A nearby OB association and H II region is visible at lower right, and another SNR (MF 15) is visible at the upper right on both [S II] and Hα frames. In this figure and Fig. 2, north and east are as indicated in the F439W panel. The arrows are 5″ long.

2.2. *Optical Spectroscopy*

Moderate-resolution optical spectroscopy of the luminous NGC 6946 SNR was obtained on 1995 October 18 using the 2.4 m Hiltner Telescope at the Michigan-Dartmouth-MIT (MDM) Observatory. A modular spectrograph similar to that in use at Las Campanas Observatory was employed with a 2.″0 × 4′ slit, a 1200 line mm^{-1} 5800 Å blaze grating, and a 1024 × 1024 Tektronix CCD detector. A 4000 s exposure was taken covering the wavelength range 4660–6940 Å with 2.34 Å $pixel^{-1}$ and 1.″4 $pixel^{-1}$ spatial scale along the slit. Effective spectral resolution based on measured comparison lamp line widths was 3.93 Å at 5000 Å, or 235 km s^{-1}. The position angle of the long slit was −30° and thus cut through spiral arm emission regions to the northwest and southeast of the MF 16 region. In addition, emission from the H II region to the northwest of MF 16 (see Fig. 2), as well as faint emission from the area between this region and MF 16, can be seen in the two-dimensional representation of the long-slit spectral data. This highlights the fact that while the *HST* images show exquisite detail, they are only detecting the emission features with the very highest surface brightness in the region.

The data were reduced using standard IRAF software routines and calibrated with Hg, Ne, and Xe lamp exposures and four standard stars taken from Oke (1974), Stone (1977), and Massey & Gronwall (1990). A one-dimensional spectrum of MF 16 was carefully extracted and corrected for background sky and minor adjacent emission contamination. The calibrated and reddening-corrected spectrum is shown in Figure 6. Measured line intensities are shown in Table 1. Slight differences between this spectrum and the one shown by Blair & Fesen (1994) are due to the differing background extraction technique used here, which should be more accurate, and to the use of the Cardelli, Clayton, &

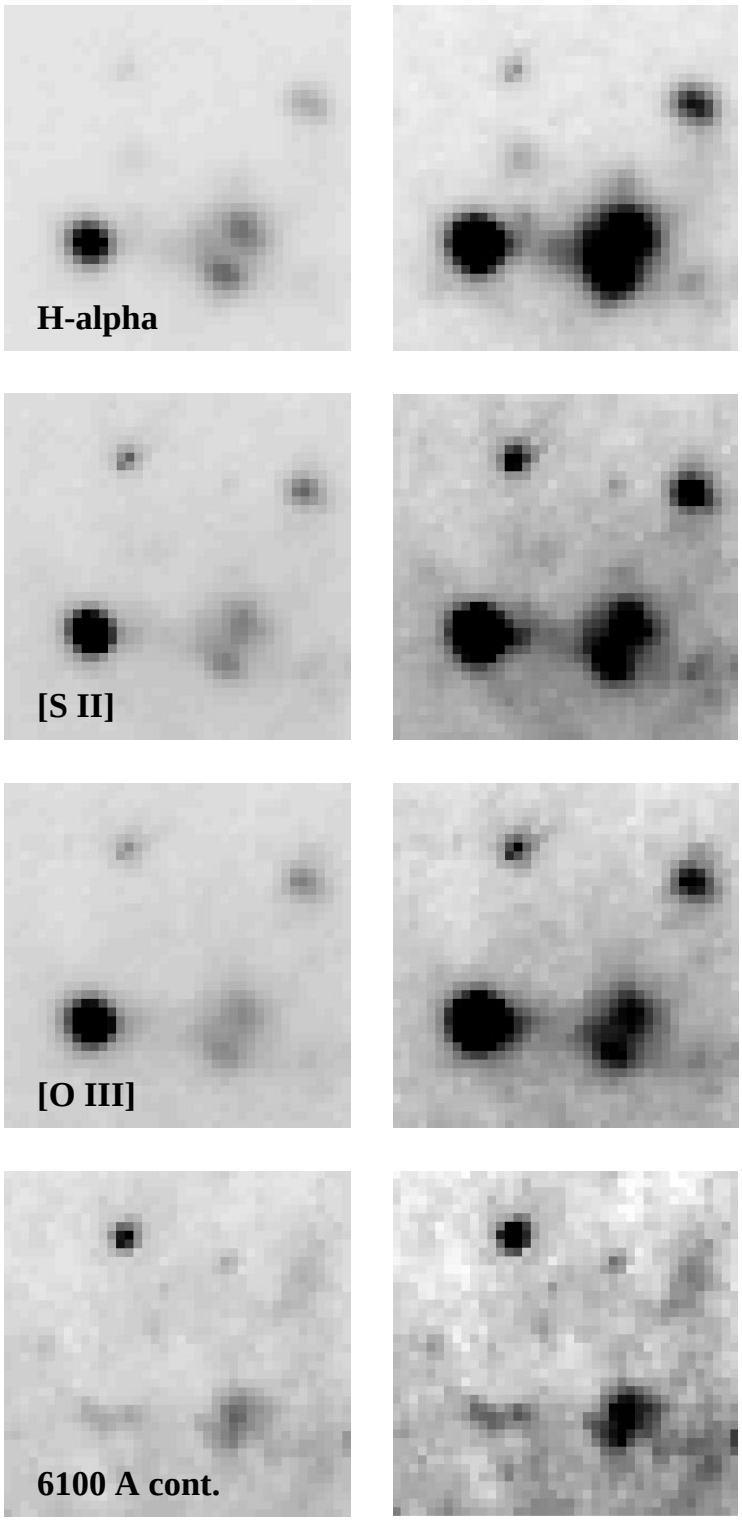

FIG. 2.—Ground-based CCD images of the region around MF 16 from the KPNO 4 m telescope (see Blair & Fesen 1994 for details). The region shown is 21″.6 square, slightly larger than the region shown in Fig. 1, and has been rotated to match Fig. 1. The labeled panels on the left are at low contrast, for direct comparison with Fig. 1; at right they are at higher contrast, showing fainter details not visible in the *HST* data.

Mathis (1989, hereafter CCM) extinction curve in this paper (compared with that of Savage & Mathis 1979 in our earlier paper). These data will be discussed further below.

3. RESULTS AND DISCUSSION

3.1. *The Stellar Component*

The continuum images from *HST* are sufficiently deep to allow us to characterize the brightest stars in the region in and around MF 16. In Figure 1 (*bottom left*), we have labeled four of the brightest, isolated stars "a"–"d," with star "d" being within the shell of MF 16 itself. These four stars are clearly visible in both the *V*-band and *B*-band *HST* images. Using calibration information from the file headers, we have derived magnitude and color information

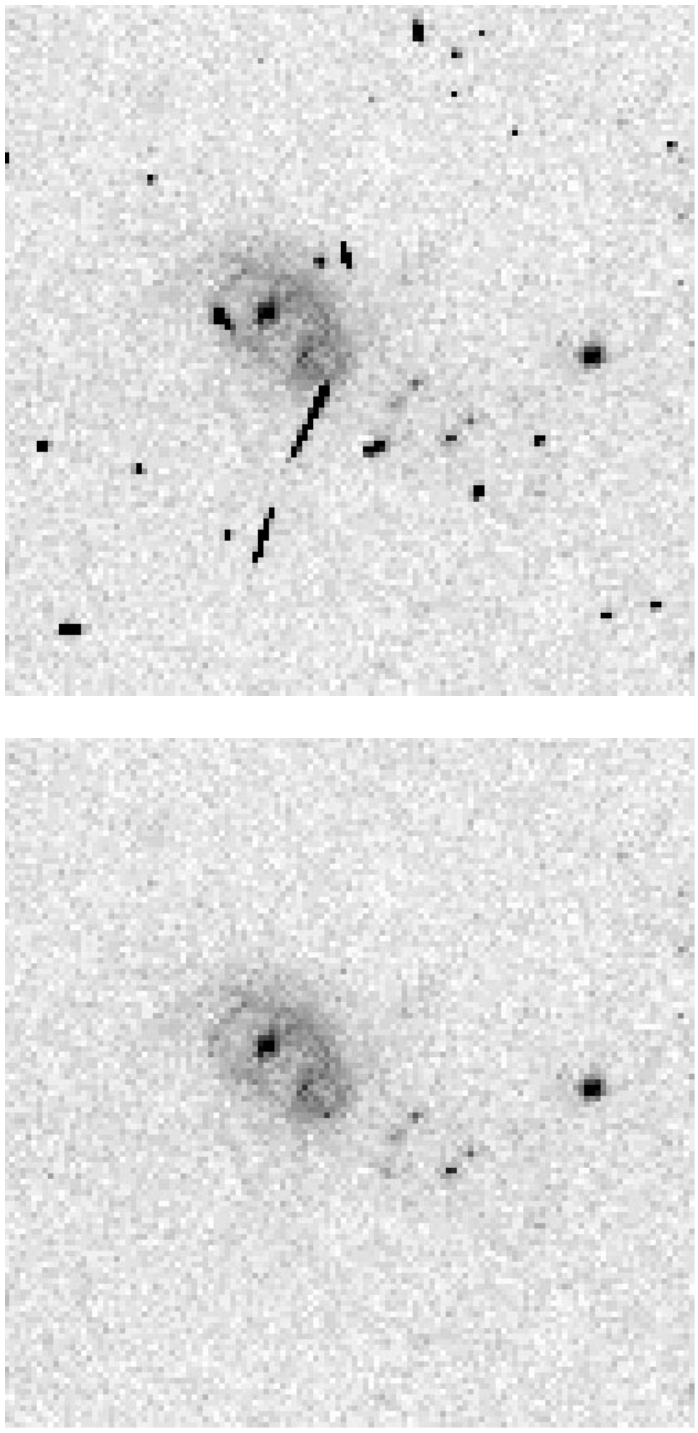

FIG. 3.—Enlargement of a 6″.2 region around MF 16 showing the effect of cosmic rays (and of their removal) in the single WFPC2 F555W frame. *Top*, original image; *bottom*, image after manual cleaning with IRAF's IMEDIT task. Note the presence of real stellar features in and around the MF 16 region.

for these stars, as listed in Table 2. We find that the magnitudes and colors of stars "a," "b," and "c" are consistent with the idea that they are typical brightest (visual) OB association members with little extinction. For instance, Mihalas & Binney (1981) list $M_V = -6.2$ and $(B-V) = -0.29$ to -0.24 for Galactic O8–B0 supergiants. This would correspond to a visual magnitude of $V = 22.34$ at $d = 5.1$ Mpc, comparable to the observed values (see Table 2).

Somewhat in contrast, star "d" is much redder. However, its V magnitude is comparable to that of the other stars and may even be brighter (although the photometry is complicated by the presence of the [O III] emission in the F555W frame), so it is plausibly very similar to stars "a," "b," and "c" but more heavily reddened. This points to fairly heavy and local extinction in the MF 16 region. The faint stars just to the west of MF 16, visible in F555W, are not detected in F439W. Deeper, more complete photometry of the stellar component in this region would permit us to better elucidate the characteristics of the local stellar population. However, because we are only detecting the brightest stars, it is possible that the MF 16 region includes a substantial

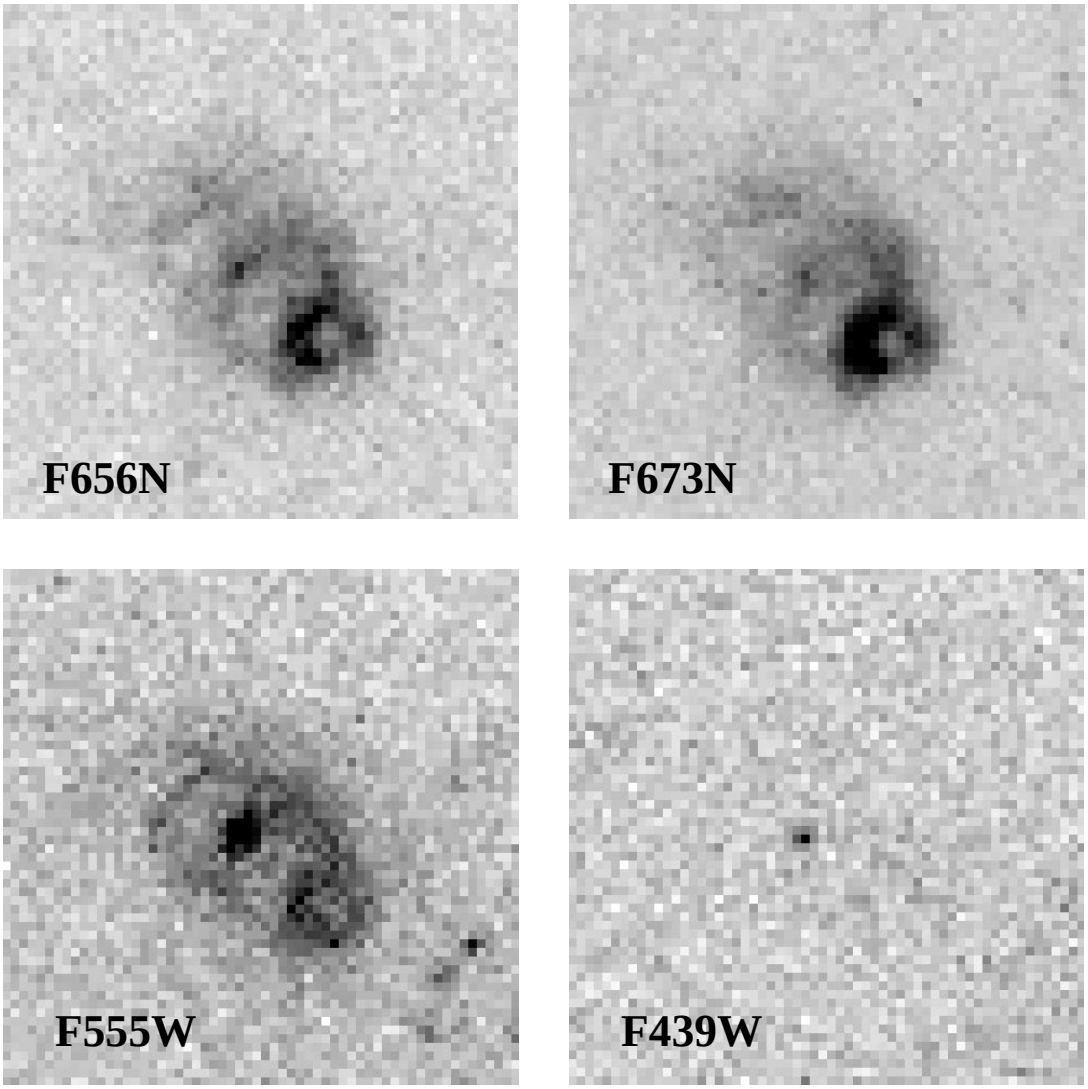

FIG. 4.—Enlargements of the region immediately surrounding MF 16 from the WFPC2 data, scaled to show details of the nebular structures. Panels and orientation are the same as in Fig. 1, but the region shown is just 3.″0 square. Note the similarity in appearance between the Hα and [S II] images, demonstrating nearly constant [S II]:Hα ratio over the structure, and the differing appearance in F555W. (The nebular emission in F555W is attributed to [O III] λ5007.)

but moderately reddened OB association that is just at the limit of detectability in the current data set.

3.2. *The Nebular Component*

Figures 1 and 2 can be used to place the nebular component in context with its surroundings. A photoionized emission region lies 9″ northwest of the SNR, about 220 pc in linear projection. This H II region can be seen on both image sets (Figs. 1 and 2), but it is better seen in the ground-based images, and it has an associated star cluster most readily seen in the F555W image. The nebular emission from the H II region seems to be double, but the OB association shows no such bifurcation. The stellar association occupies a region at least 50 pc in diameter and appears to have either an extension to the southeast in the direction of MF 16 or a separate, poorer, more heavily extincted cluster close to MF 16.

The second, fainter SNR (MF 15) appears as a faint loop of emission and is most readily visible in the [S II] exposure (see Figs. 1 and 2). This object was noted by Blair & Fesen (1994) as another probable SNR in NGC 6946, and its SNR nature was confirmed by Matonick & Fesen (1997). The roughly circular limb-brightened shell is about as bright in [S II] as in Hα; a few stars, fainter than those listed in Table 2, are visible in this region in the F555W frame (see Fig. 1). The diameter of this shell is approximately 1.″3, or 32 pc at the assumed 5.1 Mpc distance. This remnant's surface brightness, though relatively bright compared with other SNRs in NGC 6946 (Matonick & Fesen 1997), is nearly an order of magnitude lower than that of MF 16.

As can be seen from Figures 4 and 5, the MF 16 nebula is extended in an east-west direction, with overall dimensions of 1.″4 × 0.″8, or 34 pc × 20 pc, roughly similar in scale to the Cygnus Loop in our Galaxy (cf. Blair et al. 1999). What was just a single bright spot of emission seen in ground-based images is now resolved into a complex region of several distinct shells, all of which exhibit strong [S II] emission relative to Hα, indicative of collisional heating.

A bright, nearly circular ringlike feature, which we call "loop 1," is seen at the western edge of the emission

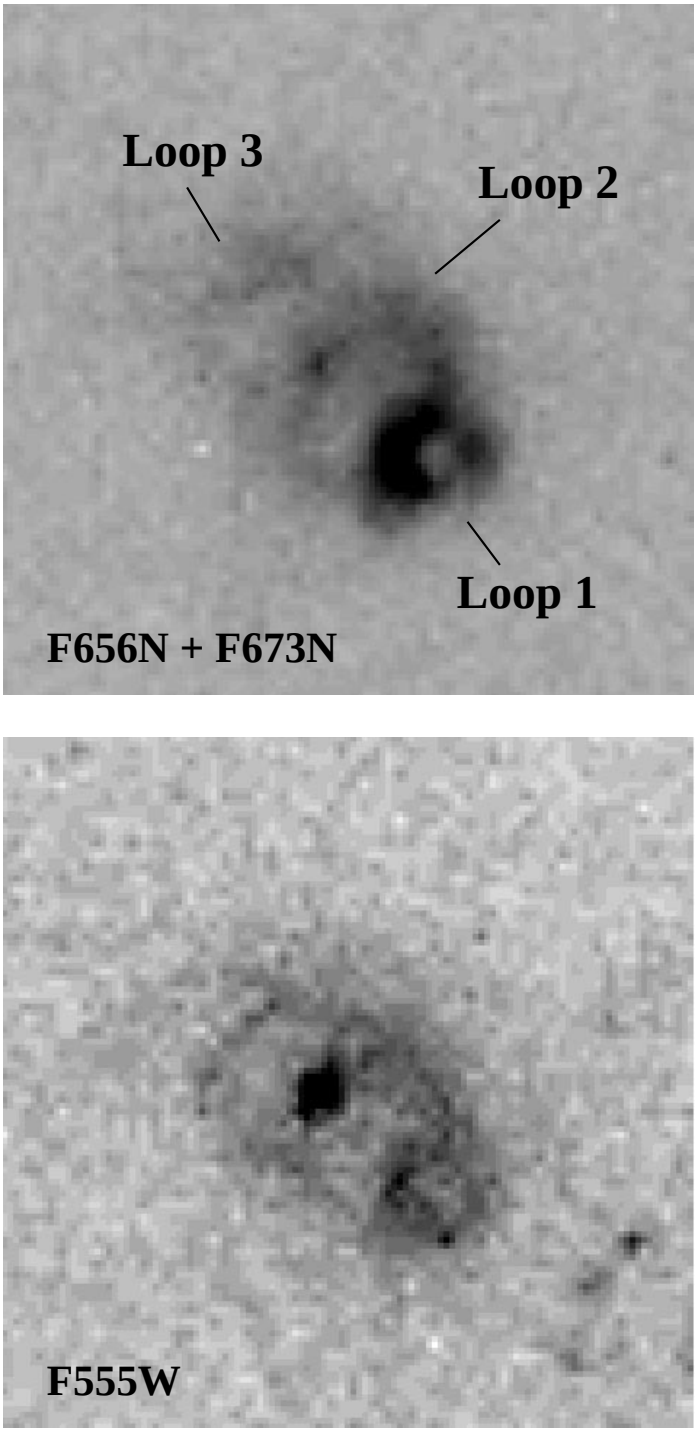

FIG. 5.—*Top*, Hα and [S II] images combined to increase the signal-to-noise ratio and subsampled to reduce the effects of pixelation;. *bottom*, subsampled version of the F555W image for comparison. The region shown is 3.″0 square, and orientation is the same as Fig. 1.

complex. It has a diameter of $\simeq 0.''35$, corresponding to ~ 9 pc. Loop 1 exhibits a very bright and well-defined southeastern limb or crescent in both the [S II] and Hα images. Loop 1 also appears in [O III] $\lambda\lambda$4959, 5007 line emission, as indicated by the F555W image, but with a more uniform appearance. Because this emission is leaking through the wing of the broad F555W filter it looks quite faint, but this is deceiving. Given the tremendous [O III] luminosity in the ground-based data (cf. Fig. 2), it is more likely that loop 1 is uniformly *bright* in [O III] but shows only marginal differential brightening in the crescent region (see especially Fig. 5).

A second, lower surface brightness but larger emission loop, "loop 2," is located just east of loop 1. It appears roughly circular, and it has a diameter of $\sim 0.''8$ (20 pc). Loop 2's western limb coincides in projection with loop 1's bright crescent. A still fainter and more easterly emission loop, "loop 3," can also be seen, but it is more poorly defined. For the part that is visible, a dimension roughly comparable to loop 2 is indicated. It is not clear whether

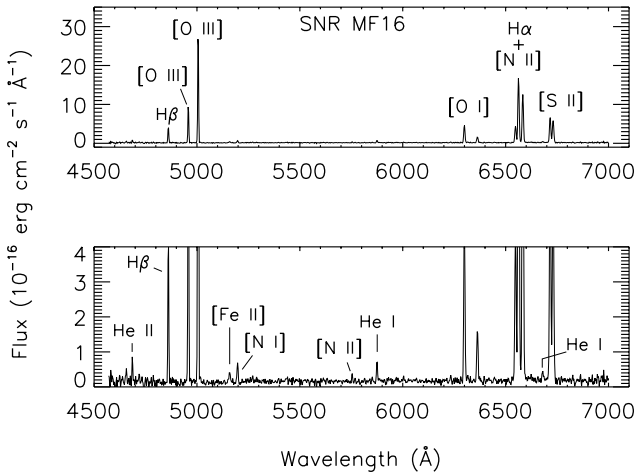

FIG. 6.—Dereddened optical CCD spectrum of the MF 16 complex in NGC 6946, obtained at MDM Observatory's 2.4 m Hiltner Telescope, in Arizona. *Top*, overall spectrum; *bottom*, magnified vertical scale for inspection of the fainter lines. No broad components are seen in these low-resolution data.

loop 2 and loop 3 are distinct structures or two portions of the same extended nebulosity. The extent of the entire loop 2 plus loop 3 structure is thus about 20 pc by 30 pc.

The [O III] λλ5007, 4959 emission of this outer multishell complex reveals a morphology somewhat different from that seen in Hα and [S II] (see Figs. 4 and 5). The [O III] image shows an elliptical east-west shell that has a sharper, more well-defined structure. Emission from the central crossing section of loop 2 may be largely missing, although this interpretation is complicated by the presence of star "d," which can be seen in the continuum exposures, particularly F555W. The overall size of the east-west shell structure seen in [O III], including loop 1, is 15 pc × 34 pc, somewhat narrower along the minor axis than its appearance in Hα and [S II]. The shell walls appear thin and are only marginally resolved in this PC1 image, implying a thickness of $\simeq 1$ pc or less. Lastly, the PC1 images show faint, diffuse emission outside the [O III] shell extending some 0.″1–0.″2 toward the east and north, especially visible in higher contrast (see Fig. 5). This is reminiscent of the photoionized cavity wall and shock precursor emission seen in the LMC remnant N132D (Morse et al. 1996), which is on a similar physical scale.

TABLE 1

LINE INTENSITIES FOR THE LUMINOUS SNR IN NGC 6946

Line	$F(\lambda)$ (Hβ = 100)	$I(\lambda)$ (Hβ = 100)[a]
He II λ4686	14	15
Hβ λ4861.....	100	100
[O III] λ4959.....	225	222
[O III] λ5007.....	685	680
[Fe II] λ5158.....	11	9
[N II] λ5199	16	13
[N II] λ5755	6	4
He I λ5876	15	9
[O I] λ6300	150	85
[O I] λ6364	55	30
[N II] λ6548	155	80
Hα λ6563.....	580	300
[N II] λ6583	445	230
He I λ6678	10	5
[S II] λ6716	240	118
[S II] λ6731	220	110

[a] Reddening correction assumes $E(B-V) = 0.65$, $A_V/E(B-V) = 3.1$, and the Cardelli et al. 1989 extinction curve.

TABLE 2

THE STELLAR COMPONENT NEAR MF 16

Star ID[a]	V	$B-V$
a	23.22	−0.18
b	23.08	−0.24
c	22.59	−0.18
d	22.64	+0.46

[a] Stars are those indicated in Fig. 1.

3.3. *Line Ratios and Kinematics*

The three Hα and [S II] emission loops exhibit line ratios highly suggestive of shock emission and hence of an SNR origin. The relative intensity of [S II] and Hα is high throughout the nebular regions and varies only slightly with position. We have extracted background-subtracted counts from the whole nebula and from various portions in the Hα and [S II] images to study this in detail. Scaling the observed counts for the whole nebula in these images by the calibrated spectral data, we find [S II]:Hα = 1.03 in loop 1 and 1.15 in the bright crescent region only, compared with 0.86 in most of the extended loop 2 and loop 3 structure. These values are much higher than those seen in photoionized nebulae, strongly suggesting that shock ionization dominates the Hα and [S II] emission from the entire nebular complex, although a contribution from photoionization is probable, especially for Hα (see below).

From the summed Hα and [S II] image data in Figure 5, we can estimate the fraction of light coming from the different components. Using background-subtracted data, we find (somewhat contrary to appearances) that roughly 30% of the light arises from loop 1 (15% from the bright crescent region alone) and 70% from loops 2 and 3 plus the diffuse outer emission. Hence, despite the appearance based on surface brightness, the largest portion of the optical *luminosity* of the MF 16 complex arises from the larger, more extended SNR structures. The tremendous luminosity of this object reported earlier is a *global* characteristic of MF 16 and is not due to a single component.

The optical ground-based spectrum we show in Figure 6 represents an average spectrum of the MF 16 region, there being insufficient spatial resolution to provide information on any substructure in MF 16 itself. The extinction is $E(B-V) = 0.65$, as derived from the observed Balmer decrement, a CCM extinction curve, and an assumed theoretical Hα:Hβ ratio of 3.0 [Note that this is higher than the $E(B-V) = 0.52$ derived by Blair & Fesen 1994 from earlier data; see § 2.2]. Correcting the stellar color of star "d" for the observed extinction makes it consistent in color with the other stars shown in Table 2, strengthening the idea that star "d" is physically associated with MF 16, and that the increased extinction is relatively local to MF 16.

The electron density sensitive [S II] line ratio of λ6716/λ6731 is among the highest values for SNRs in NGC 6946, as well as in several other nearby galaxies (Blair & Long 1997; Matonick & Fesen 1997; Gordon et al. 1998). These

lines will be dominated by the shocked component even if some photoionized gas is present (see below). The dereddened ratio of 1.09 indicates an electron density of 410 ± 100 cm^{-3}, assuming an electron temperature of 10^4 K. This is a very high mean density. For comparison, densities of individual Cygnus Loop filaments are nearly always in the low-density limit (<100 cm^{-3}; see Fesen, Blair, & Kirshner 1982). Although extreme clumpiness could drive this number up, the observed morphology of the nebular emission argues against this scenario. The large density in the shocked gas points toward a mean preshock density of order 10 cm^{-3} and is indicative of shock propagation into presupernova mass loss or of an otherwise dense circumstellar environment.

These low-resolution, high-S/N spectral data show no indication of faint broad wings on the bright lines, and they show little broadening above the instrumental profile. Our best limit on any high-velocity component comes from the [O III] 5007 Å line. The measured line width is 4.48 Å FWHM, or 270 km s^{-1}, but deconvolution of the instrumental profile would indicate an even smaller value. This is consistent with the higher resolution long-slit echelle data reported by Dunne, Gruendl, & Chu (2000; their Table 2).

MF 16's optical spectrum shows two other major differences with respect to other NGC 6946 SNRs (Matonick & Fesen 1997): (1) the [O III] emission is very strong with respect to hydrogen Balmer lines; and (2) the intensity of the [N II] $\lambda\lambda$6548, 6583 emission is elevated relative to Hα. Dunne et al. (2000) report two-component line profiles for [O III], Hα, and [N II]. A narrow component is attributed to photoionized gas, and a broader component ($\Delta v = 250$–285 km s^{-1} FWHM) is attributed to shocks. Using their observed ratios of fluxes in the broad and narrow components for these lines with the information listed in our Table 1, we can derive the line ratios in the broad and narrow components separately. (No observations were obtained for the [S II] lines, which should be almost completely dominated by the broader component.) For instance, the average intrinsic [O III]:Hα ratio is 3.0, but we find a ratio of only 2.60 for the broad-component gas and 3.60 for the narrow-component gas. For [N II]:Hα, we find a ratio of 1.10 for the broad component and 0.93 for the narrow component. These are subtle but important clues, which are discussed separately below.

If we assume that the broad-to-narrow ratios for Hα and Hβ are the same, we derive an [O III]:Hβ of 10.8 for the narrow component and 7.8 for the broad component. Hence, the perceived strength of the [O III] relative to the Balmer lines is partially because of the photoionized component with very high relative [O III] emission compared with steady flow shock models. However, the [O III]:Hβ ratio for the broad component is still substantial, indicative of a shock velocity well above 100 km s^{-1}, possibly in the 120–150 km s^{-1} range (Dopita et al. 1984; Hartigan, Raymond, & Hartmann 1987). This is consistent with the observed broad component widths. It is possible that the high observed ratio of [O III]:Hβ in the broad component indicates that a fraction of the shocks are "incomplete" (i.e., recent encounters with dense material that have yet to establish a full cooling and recombination zone), but this is not certain with the current data.

The [N II]:Hα ratio is often seen to be elevated in shocks compared with photoionized gas (see Blair & Long 1997). It is thus gratifying to see that the broad component has an elevated ratio compared with the narrow component after our deconvolution. However, as pointed out by Dunne et al. (2000), even the narrow [N II] emission in MF 16 has an elevated ratio compared with other NGC 6946 H II regions, and the broad-component ratio is considerably stronger than in any of the five other NGC 6946 SNRs studied by Matonick & Fesen (1997). This indicates nitrogen enrichment of the material, like that expected as a result of mass loss from young, high-mass stars, as also concluded by Dunne et al. (2000). We also note the detection of [N II] λ5755, which allows a measurement of the electron temperature in the N^+ zone; we find $T(N^+) = 10{,}500 \pm 800$ K, another indication that shock heating is substantial.

Unfortunately, relating the kinematic components to specific regions seen in the *HST* images cannot be done with certainty with the current data. In particular, whether the narrow (photoionized) component is associated with stellar photoionization or with photoionized shock precursor emission as seen outside the cavity wall in N132D (Morse et al. 1996) remains to be determined.

4. INTERPRETATION

The new *HST* images have greatly clarified the nature of the unusual SNR MF 16 in NGC 6946 by resolving it into a complex region of nebular shells and a possible associated young star cluster. Some tentative conclusions can be drawn based on the observed morphology seen in the *HST* images and on the supporting data. We find the circular appearance of loop 1 and the associated brightened crescent of emission to be compelling evidence that loop 1 represents a relatively young, physically distinct SNR caught in the act of interacting with the shell of an older expanding shell from an earlier explosion (loop 2). It is not clear, however, whether loop 3 represents yet another SNR or is simply an extension of the older SNR represented by loop 2.

Comparison of MF 16's Hα flux with that of other NGC 6946 SNRs shows that it is about 3 times as bright as the next brightest SNR and more than an order of magnitude brighter than the mean of the SNRs in the sample of Matonick & Fesen (1997). It is worth noting that, at 5.1 Mpc, the current sample of optical SNRs is surely biased toward the brighter objects, making MF 16's total luminosity even more extreme. The relative luminosities of the extended component (loops 2 and 3, 70%) and the loop 1 region (30%) make it clear that both of these nebulae *by themselves* would be extremely luminous by normal SNR standards. Taken in tandem, they become even more extreme. Both the high mean electron density implied by the [S II] line ratio and the strong [N II] $\lambda\lambda$6548, 6583 line emission relative to Hα suggests shock interaction with nitrogen-enriched circumstellar material. This is consistent with MF 16's location within or near a young stellar association, and the enriched material could be attributable to the direct progenitor(s) responsible for MF 16 or to other massive stars in the region.

The appearance of the MF 16 nebula in [O III] (from the F555W image) is suggestive of a young windblown cavity. The presence of multiple Hα and [S II] loops or shells projected within the [O III] cavity suggests coeval evolution of two or more massive association members that then exploded within a relatively short time period, still within a fairly young and dense interstellar-medium and circumstellar-medium environment. The high extinction local to the MF 16 region permits only the brightest

members of the local population to be seen in the current *HST* images. The centers of the loop 1 and loop 2 regions are separated by 0.″36, or 8.9 pc in linear dimension on the sky (hence placing a lower limit on the separation of the progenitors in the multiple-explosion model). The presence of star "d" in projection within the MF 16 shell strongly suggests the presence of massive progenitor stars in the region. Both the interaction region of loops 1 and 2 and the high density of the cavity walls are the chief causes of MF 16's extraordinary optical, radio, and X-ray luminosities.

One of the ramifications of the tremendous luminosity of MF 16 is that either the effective age of the SNR complex must be small or the explosive energy input was high (or some combination of the two). Blair & Fesen (1994), for instance, estimated the age to be less than 3500 yr if the explosion energy was $\sim 10^{51}$ ergs and the current observed luminosity was representative over the lifetime of the object. Having multiple explosions could in principle be a contributing factor, providing more than a single supernova's energy input into the region. However, an extreme explosion energy or "hypernova" picture (see Wang 1999) does not appear to be necessary to explain MF 16 (see, e.g., Dunne et al. 2000).

If our interpretation of the elliptical [O III] ring is correct, the larger, older SNR is in a cavity blown by the precursor star. Hence, this SNR could have expanded rapidly, depositing its energy only after reaching the cavity wall. Thus, its moderate size (20 pc × 30 pc) could be accounted for by an SNR only a few thousand years old, much younger than one would estimate from a Sedov model and assumptions of a homogeneous surrounding medium ($\sim$25,000 yr; Dunne et al. 2000). The SNR N132D in the LMC is a good comparison. This object has been interpreted as a cavity explosion with an outer shell of diameter 23 pc, but with a kinematically determined expansion age (from the ejecta) of only 3150 yr (Morse, Winkler, & Kirshner 1995; Morse et al. 1996). This interpretation for MF 16, however, requires that the smaller loop 1 SNR be more nearly coeval with the SNR that created the larger loop 2 and/or loop 3 structure, presumably with at least two SNe in the same region within a few thousand years of each other.

The current data set leaves us with a number of important questions to answer. Is the apparent morphology really representative of multiple shells of interacting SNRs? Does patchiness in overlying extinction affect the observed morphology? To what regions are the differing kinematic components observed by Dunne et al. (2000) attributed? Is the bright crescent really a region of interaction, or just a projection effect or geometric fluke? Long-slit spectroscopy at high spatial resolution could clarify the extinction, kinematics, and relative line intensities for the various components and permit a clear answer to these questions.

In addition, further *HST* imaging will be important. Because our understanding of the nebula's [O III] structure was derived from its [O III] λ5007 emission leaking through the wing of a broadband filter, it would be beneficial to obtain a deeper exposure using a narrowband [O III] filter to better elucidate the structure of the [O III] nebular emissions. Deeper broadband imagery could provide a much better understanding of the underlying stellar population near MF 16 and strengthen our tentative conclusion that we are seeing only the brightest members of a larger association.

We wish to thank A. Hurford for assistance obtaining the MDM spectral data and You-Hua Chu for discussions of her long-slit echelle observations of MF 16 prior to publication. This work has been supported by STScI grant GO-06118.01-94A and GO-7289.01-96A to Johns Hopkins University.

REFERENCES

Blair, W. P., & Fesen, R. A. 1994, ApJ, 424, L103
Blair, W. P., Kirshner, R. P., & Winkler, P. F., Jr. 1983, ApJ, 272, 84
Blair, W. P., & Long, K. S. 1997, ApJS, 108, 261
Blair, W. P., Sankrit, R., Raymond, J. C., & Long, K. S. 1999, AJ, 118, 942
Cardelli, J. A., Clayton G. C., & Mathis, J. S. 1989, ApJ, 345, 245 (CCM)
Cowan, J. J., & Branch, D. 1985, ApJ, 293, 400
de Vaucouleurs, G. 1979, ApJ, 227, 729
de Vaucouleurs, G., de Vaucouleurs, A., & Corwin, H. G., Jr. 1976, Second Reference Catalogue of Bright Galaxies (Austin: Univ. Texas Press)
Dopita, M. A., Binette, L., D'Odorico, S., & Benvenuti, P. 1984, ApJ, 276, 653
Dunne, B. C., Gruendl, R. A., & Chu, Y.-H. 2000, AJ, 119, 1172
Fesen, R. A., Blair, W. P., & Kirshner, R. P. 1982, ApJ, 262, 171
Gordon, S. M., Kirshner, R. P., Long, K. S., Blair, W. P., Duric, N., & Smith, R. C. 1998, ApJS, 117, 89
Hartigan, P., Raymond, J., & Hartmann, L. 1987, ApJ, 316, 323
Liller, W. 1990, IAU Circ. 5091
Long, K. S., Blair, W. P., Kirshner, R. P., & Winkler, P. F. 1990, ApJS, 72, 61
Massey, P., & Gronwall, C. 1990, ApJ, 358, 344
Matonick, D. M., & Fesen, R. A. 1997, ApJS, 112, 49
Mihalas, D., & Binney, J. 1981, Galactic Astronomy (2d ed.; New York: Freeman)
Morse, J. A., et al. 1996, AJ, 112, 509
Morse, J. A., Winkler, P. F., & Kirshner, R. P. 1995, AJ, 109, 2104
Oke, J. B. 1974, ApJS, 27, 21
Savage, B. D., & Mathis, J. S. 1979, ARA&A, 17, 73
Schlegel, E. M. 1994, ApJ, 424, L99
Stone, R. P. S. 1977, ApJ, 218, 767
Van Dyk, S. D., Sramek, R. A., Weiler, K. W., Hyman, S. D., & Virden, R. E. 1994, ApJ, 425, L77
Wang, Q. D. 1999, ApJ, 517, L27